RSC Advances

ROYAL SOCIETY OF CHEMISTRY

www.rsc.org/advances

RSC Advances

RSCPublishing

Paper

New insights on the relationship between the photocatalytic activity and TiO_2-GR Composites

Cite this: DOI: 10.1039/x0xx00000x

Yanyan Zhu[a, b‡], Yajun Wang[c ‡], Wenqing Yao[a], Ruilong Zong[a], Yongfa Zhu[a*]

Received ooth January 2015,
Accepted ooth January 2015

DOI: 10.1039/x0xx00000x

www.rsc.org/

Abstract: TiO_2-graphene (TiO_2-GR) composites were synthesized via hydrothermal methods in ethanol-water solvent. The photocatalytic oxidation, photocatalytic reduction and photoelectrochemical properties were systematically investigated to explore the real role of graphene in TiO_2-GR composite photocatalysts. The pollutant degradation and adsorption results strongly manifested the composited graphene in TiO_2-GR can't enhance the photocatalytic oxidation activity of degrading pollutant. The migration process of photo-generated holes in the photocatalytic oxidation reaction is the rate-determining step, which can't be promoted by the composited graphene in TiO_2-GR. However, composited graphene can promote the migration of photo-generated electrons in TiO_2-GR due to its excellent conductivity, which mainly enhances the performance of H_2 evolution and photoeletrochemical properties.

1. Introduction

Graphene has attracted widespread attention due to its outstanding mechanical, thermal, optical, and electronic properties.[1] Graphene possesses excellent electron mobility, extremely theoretically high surface area and strong adsorption capacity for organic pollutants and metal ions.[2, 3] Recently, graphene has been used to enhance the photocatalytic performance. Many graphene-based photocatalysts have been reported, such as CdS-graphene,[4-6] TiO_2-graphene,[7-10] ZnO-graphene[11, 12] and so on. The graphene has been regarded to enhance the phtocatalystic oxidation and photocatalytic reduction of many semiconductor photocatlysts as a very good cocatalyst. Many reports have shown that the combination of graphene with photocatalysts can enhance the photocatalytic activity on the degradation of organic pollutant.[4, 7-12] A view is commonly regarded: graphene can quickly separate and transfer the photo-generated electrons from the conduction band of photocatalysts and further enhance the photocatalytic oxidation and photocatalytic reduction. As is well known, graphene as a carbon material with high specific surface area could strongly adsorb many organic pollutants during photocatalytic reaction process, which would affect the evaluation of graphene-based composite photocatalysts.[9, 13-16] In many reported works, dyes (methylene blue (MB), methyl orange, rhodamine B and so on) are chosen as probes to evaluate the photocatalytic activity,[4, 7, 8, 10]meanwhile the strong adsorption effect of graphene for pollutant was neglected. The strong adsorption of graphene for pollutant will result in great difference of the pollutant's initial reaction concentration. [7, 8, 17] The remaining concentration of MB over TiO_2 was about 4.4 times as high as that over TiO_2-10%GO after adsorption-desorption equilibrium.[18] In this situation, the evaluation of photocatalytic activity over TiO_2 and TiO_2-10%GO might be no objective. Moreover, the photocatalytic performance of TiO_2-GR gradually decreased during several reaction cycles, only 53% of its photocatalytic performance remained after five cycles of photocatalytic reaction.[13] On the contrary, TiO_2 usually maintains better stability on the photocatalytic degradation of pollutants.[14, 16] The above results indicate that the high phtocatalytic oxidation performance of TiO_2-graphene may be due to the strong adsorption effect of graphene for pollutant rather than photocatalytic degradation. It is worth pointing out that different initial reaction concentration of pollutants will lead to great difference of photocatalytic reaction apparent rate constant k and C/C_0.[19] The lower initial reaction concentration of pollutant is, the higher calculated apparent rate constant k is. However, there is no report regarding the influence of strong adsorption of graphene on pollutant's initial reaction concentration and photocatalytic activity of graphene-based photocatalysts. Therefore, in many works, the explanations for the role of graphene maybe have some mistakes because the effect of strong adsorption of graphene for pollutant was not taken into account.

Moreover, in photocatalytic reduction, many researches highlight that the introduction of graphene can improve the

photocatalytic H_2 evolution.[6, 20-22] Yu and co-workers prepared CdS-graphene composites and found that CdS-graphene composites exhibited higher H_2 evolution rate and higher quantum efficiency than pure CdS.[23] Thus, key fundamental issues are naturally questioned. Can graphene really enhance photocatalytic activity?

In this work, TiO_2-GR composites were synthesized via hydrothermal method in ethanol-water solvent.[7, 8] Photocatalytic degradation activity of pollutants, photocatalytic H_2 evolution performance from water splitting and photoeletrochemical properties were systematically investigated. The real role of graphene in photocatalytic oxidation has been examined by eliminating the strong adsorption effect of graphene for pollutant.

2. Experimental

2.1 Preparation of TiO_2-GR Samples

GO was prepared from natural graphite via a modified Hummers method.[24] The GO solution was obtained through the dispersion of mixture into water and its concentration was calculated by drying 100 g GO solution. TiO_2-GR composites were prepared via solvent-thermal method according to literature.[7, 8] The appropriate amount of 0.523% GO solution was added into 150 mL ethanol-water (ethanol: deionized water= 1:2 v/v). Then 1.0 g Degussa TiO_2 was added into the mixture and vigorously stirred at room temperature for 2 h. The above solution was transferred into a 200 mL autoclave and maintained at 120 °C for 24 h to achieve the reduction of GO and the deposition of TiO_2 onto the graphene sheet. Finally, the resulting composite was washed by deionized water several times and dried at 60 °C. Then, TiO_2-GR composites with different weight ratios of graphene were obtained.

2.2 Photocatalytic Experiment

The photocatalytic oxidation activities were evaluated on the degradation of methylene blue (MB) and phenol under 254 nm UV light. 25 mg photocatalyst was totally dispersed in a 100 mL aqueous solution of MB (11.2-37.4 ppm) or phenol (10-50 ppm). Before irradiation, the suspensions were magnetically stirred in the dark for 4 h to get adsorption-desorption equilibrium. A 3.0 mL aliquots were sampled at certain time intervals during the experiment and centrifuged to remove the photocatalysts completely. The solution was analyzed on a Hitachi U-3010 UV-Vis spectrophotometer to get the concentration of MB. The concentration of phenol was analyzed by a High-Performance Liquid Chromatography (Lumtech HPLC) system, using a UV detector operated at 270 nm. The mobile phase was methanol and deionized water (60:40 v/v) and its flow rate was 1.0 mL/min. The oxidative species in the photocatalytic system could be examined through the trapping by tert-butyl alcohol (t-BuOH, hydroxyl radical scavenger), ethylenediaminetetraacetic acid disodium salt (EDTA-2Na, hole scavenger) and N_2 (superoxide radical scavenger).

In the photocatalytic H_2 evolution, 0.2 g photocatalyst was dispersed in a 100 mL 15% (v/v) mixed methanol-water solution under 250～380 nm UV irradiation. The amount of evolved H_2 was detected by a gas chromatograph equipped with a thermal conductivity detector (TCD).

2.3 Characterization

UV-Vis diffuse reflectance spectra (DRS) of the samples were measured from a Hitachi U-3010 UV-Vis spectrophotometer. Transmission electron microscopy (TEM) images were obtained on a Hitachi HT7700 electron microscope operated at an accelerating voltage of 100 kV. Raman spectra were measured by an HR800 confocal Raman microscopy (Horiba) in the range of 200–2000 cm^{-1}. The Brunauer-Emmett-Teller (BET) surface area and pore size distribution were measured by ASAP 3020 instrument from Micromeritics.

The photocurrent and electrochemical impedance spectra (EIS) were measured on an electrochemical system (CHI-660B, China) using a standard three-electrode cell under a 11 W germicidal lamp at the wavelength of 254 nm. The ITO/sample with 20 mm×45 mm was acted as the working electrode, a platinum wire was acted as the counter electrode and a standard calomel electrode (SCE) was acted as reference electrode. The ITO/sample was prepared by a dip-coating method: 6 mg photocatalyst was suspended in 0.75 mL ethanol to make slurry by ultrasonic treatment, and then was dip-coated onto ITO glass electrode. The as-prepared electrodes were dried under ambient conditions for about 12 h, and then calcined at 120 ℃ for 5 h in air. The electrolyte solution was 0.1 M Na_2SO_4, and potentials are given with reference to the SCE. The photoelectric responses of the as-prepared photocatalysts with the light on and off were measured at 0.0 V. Electrochemical impedance spectroscopy (EIS) was carried out at the open circuit potential, and a sinusoidal ac perturbation of 5 mV was applied to the electrode over the frequency range of 0.05–10^5 Hz.

3. Results and discussion

3.1 Intrinsic role of graphene on photocatalytic performance of TiO_2-GR

Graphene has good selective adsorption ability for many organic pollutants such as dyes as high BET carbon material.[25] The adsorption and degradation performance of MB over TiO_2 and TiO_2-GR composites were investigated in various MB initial concentrations (Fig.1 and Fig.S1-Fig.S3). Before irradiation, the suspensions were stirred in the dark for 4 h to get the adsorption-desorption equilibrium. As is well known, the photocatalytic oxidation process is fit to pseudo-first-order kinetics.[26] When the initial concentration of MB is low (3.7 ppm, Fig.1a), the remaining MB concentration (initial reaction concentration of MB) in solution over TiO_2, TiO_2-1%GR, TiO_2-5%GR and TiO_2-10%GR are 3.4 ppm, 2.5 ppm, 1.5 ppm and 1.1 ppm after reaching the adsorption-desorption equilibrium in the dark. It should be mentioned that the remaining MB concentrations in TiO_2-10%GR is 1.1 ppm, which is only 0.31 times of initial MB concentration (3.7 ppm). However, the remaining MB concentration in TiO_2 is 3.4 ppm, which means the initial reaction concentrations of MB in TiO_2 system are much higher than that of TiO_2-GR composites. These great differences of MB initial reaction concentration can be observed in most previous reported works.[9, 16, 27] Apparently, a comparison of photocatalytic activity between TiO_2 and TiO_2-GR by calculating apparent rate constant k can't be made

reasonably under this condition. More importantly, in photocatalytic reaction, different initial reaction concentration of the pollutant would result in different calculated apparent rate constant k. The lower initial reaction concentration of MB is, the higher calculated apparent rate constant k is.[19, 28] Therefore, TiO_2-1%GR, TiO_2-5%GR and TiO_2-10%GR show higher apparent rate constants and better photocatalytic performance than TiO_2.[13, 14, 16] At the meantime, excess black graphene would absorb a lot of light and inhibit the efficient absorption of photons by TiO_2 in the TiO_2-10%GR system. The TiO_2-5%GR composite shows the best photocatalytic performance with a maximal apparent rate constant k of 0.234 min^{-1}, which is 76% higher than that of TiO_2 (0.133 min^{-1}). Analogous results are also observed in other low initial MB concentrations (11.2 ppm and 18.7 ppm) and the results are shown in Fig.S1 and Fig.S2.

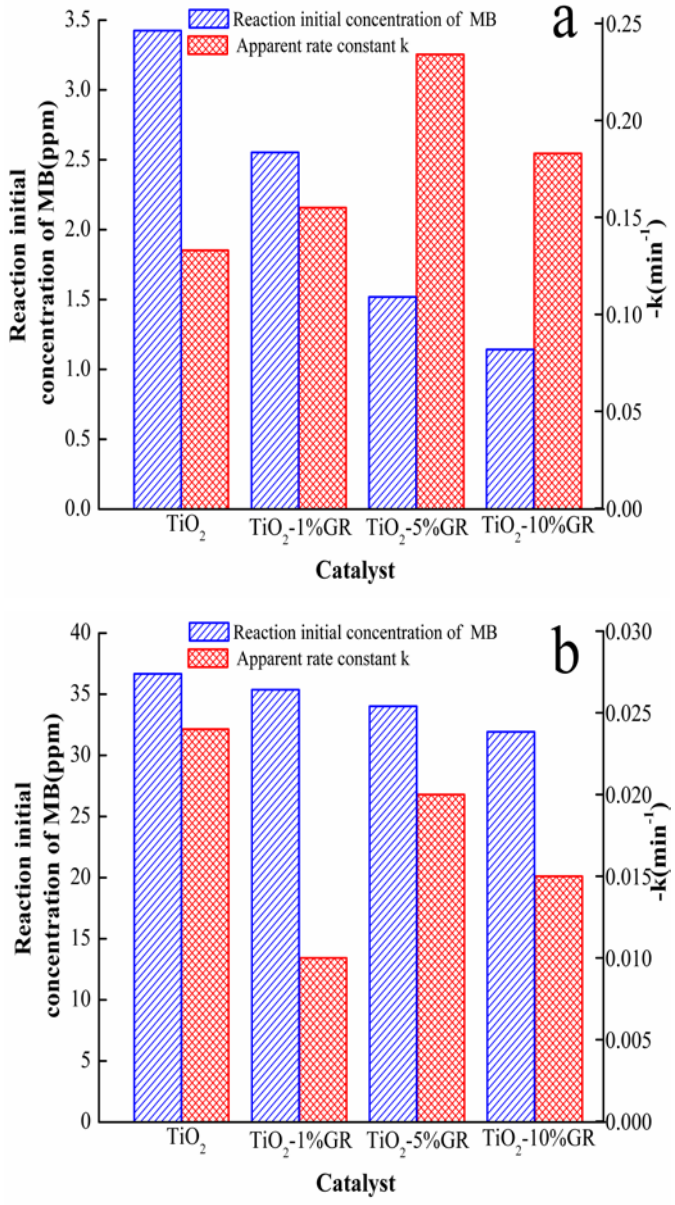

Fig.1 The adsorption and photocatalytic oxidative degradation performance of MB over TiO_2 and TiO_2-GR composites, (a) MB initial concentration: 3.7 ppm, (b) MB initial concentration: 37.4 ppm. (blue bar: reaction initial concentration of MB after adsorption-desorption equilibrium, red bar: apparent rate constant k. The suspensions were stirred in the dark for 4 h to get adsorption-desorption equilibrium, the light intensity of 254 nm UV light is 0.9 $mW{\cdot}cm^{-2}$)

When the initial concentration of MB is high (37.4 ppm, Fig.1b), the remaining MB concentrations in solution over TiO_2, TiO_2-1%GR, TiO_2-5%GR and TiO_2-10%GR after adsorption-desorption equilibrium in dark were 36.7 ppm, 35.5 ppm, 34.0 ppm and 31.8 ppm, which were 0.98, 0.95, 0.91 and 0.85 times as high as the initial MB concentration. There is no obvious difference in the remaining MB concentrations between TiO_2 and TiO_2-GR composites, indicating that the pollutant's initial reaction concentrations are almost the same. At this time, the photocatalytic activities of TiO_2-GR composites are not higher than that of TiO_2. Analogous results can be obtained in another high initial MB concentration reaction (29.9 ppm, Fig.S3). Based on above results, a speculation can be proposed: the essential photocatalytic oxidative activity of TiO_2-GR is not higher than that of TiO_2; the higher calculated apparent rate constant k of TiO_2-GR is due to the great difference in the initial reaction concentration of MB caused by the strong adsorption of graphene. After eliminating the adsorption effect of graphene by increasing the initial concentration of MB, the calculated apparent rate constant k of TiO_2-GR composites is not higher than that of TiO_2.

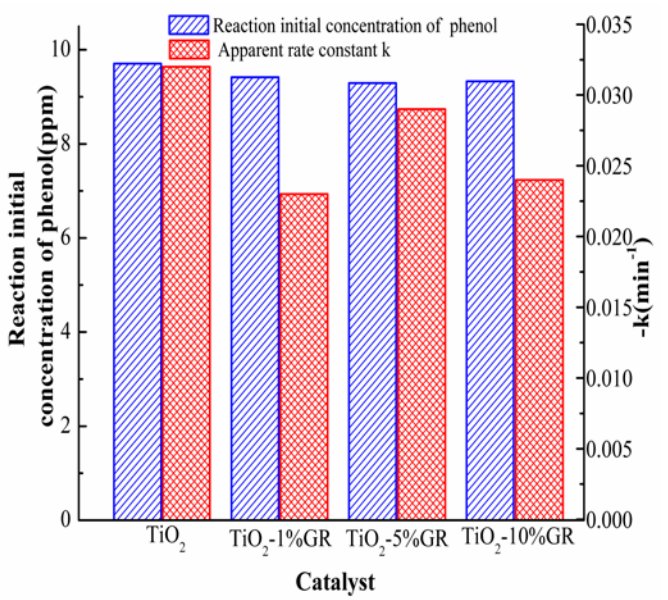

Fig.2 The adsorption and photocatalytic oxidative degradation of 10.0 ppm phenol over TiO_2 and TiO_2-GR composites (the suspensions were stirred in the dark for 4 h to get adsorption-desorption equilibrium, the light intensity of 254 nm UV light is 0.9 mW·cm-2)

Moreover, TiO_2 and TiO_2-GR composites were used to adsorb and photocatalytic degrade colorless phenol. Fig.2 shows the adsorption and photocatalytic degradation of 10.0 ppm phenol over TiO_2 and TiO_2-GR composites. After adsorption-desorption equilibrium, the remaining phenol concentrations in TiO_2 and TiO_2-GR system are basically the same, suggesting that the initial reaction concentrations of phenol are almost the same. In this case, the photocatalytic

activities of TiO_2-GR composites are lower than that of TiO_2. These results strongly highlight that the essential photocatalytic activity of TiO_2-GR is not higher than that of TiO_2 after eliminating the adsorption effect of graphene. Moreover, the phenol adsorption and photocatalytic degradation over TiO_2 and TiO_2-GR in 30.0 ppm and 50.0 ppm phenol initial concentration were also investigated and analogous results can be obtained (Fig.S4 and Fig.S5). These results further confirm our speculation: the photocatalytic activity of TiO_2-GR can't truly enhance by composited graphene when the adsorption effect of graphene for the pollution is eliminated.

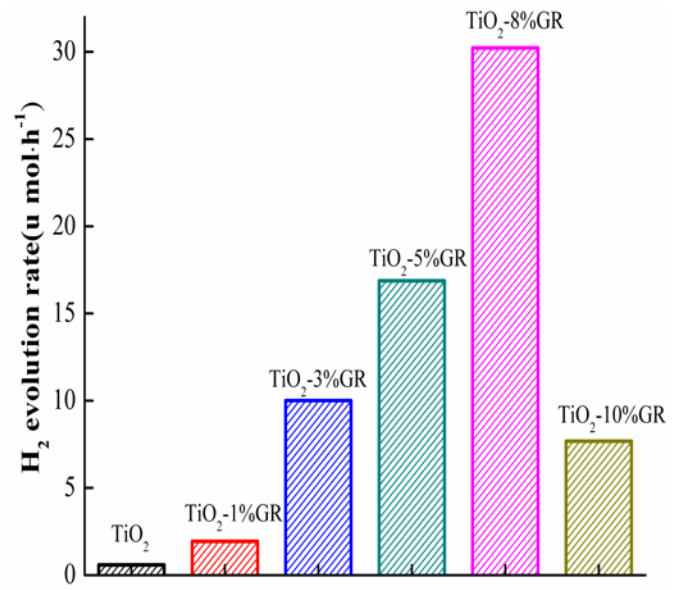

Fig.3 The photocatalytic activity of H_2 evolution over TiO_2 and TiO_2-GR composites

The H_2 evolution performance of TiO_2 and TiO_2-GR composites were evaluated to reveal the intrinsic effect of graphene on photocatalytic reduction. As shown in Fig.3, all TiO_2-GR composites show higher H_2 evolution activity than TiO_2. The H_2 evolution performance of TiO_2-GR composites first increased and then decreased with the increase of graphene loading amount. The TiO_2-8%GR composite exhibits the optimum H_2 evolution activity (30.3 μmol·h $^{-1}$), which is 51.6 times higher than that of TiO_2. However, the further increase of graphene proportion results in a decrease of the H_2 evolution activity. This is reasonable because the introduction of large proportion of graphene will reduce the contact surface of TiO_2 particles with the light irradiation, leading to a decreased photocatalytic performance. Thus, a suitable amount of graphene is important for optimizing the H_2 evolution performance of TiO_2-GR composites. The excellent electron mobility and a high surface area of graphene can effectively promote the migration of photo-generated electrons, increase the reaction space, and act as a H_2 evolution cocatalyst, leading to an enhanced H_2 evolution performance.[23, 29]

Fig.4 shows the photocurrents of TiO_2 and TiO_2-GR composites. The TiO_2-GR composites show higher photocurrent than TiO_2, and the photocurrent of TiO_2-GR composites first increases and then decreases with graphene loading amount increasing. The excellent electron mobility of graphene can effectively promote the migration of photo-generated electrons, leading to an enhanced photocurrent. TiO_2-8%GR presents the highest photocurrent, which is consistent with the H_2 evolution performance.

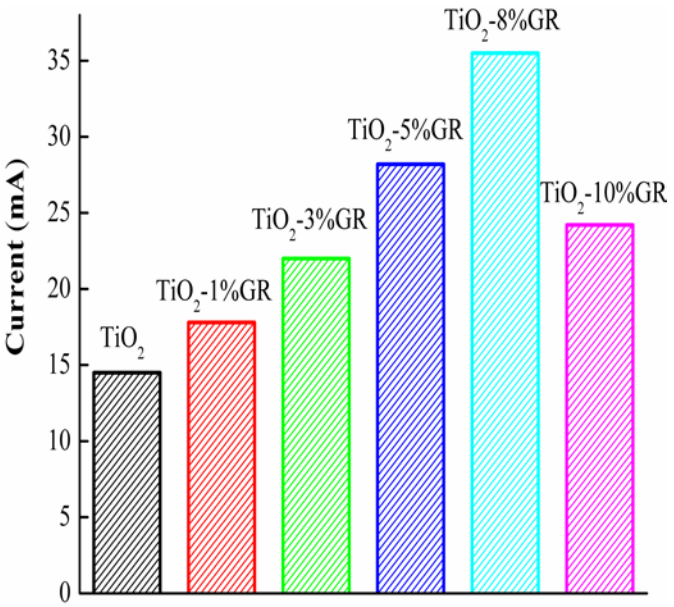

Fig.4 The photocurrent of TiO_2 and TiO_2-GR composites under 254 nm UV light irradiation

3.2 Mechanism of photocatalytic reaction

On the basis of the results for degradation of MB and phenol, we argue that composited graphene can't really enhance the photocatalytic oxidation activity of TiO_2. The higher apparent rate constant k of TiO_2-GR composites is due to the lower reaction initial concentration caused by strong adsorptivity of graphene for pollutants. EIS spectra and main oxidative species detection were performed to investigate the intrinsic role of graphene in TiO_2-GR composites. Fig.5 shows the EIS Nyquist plots of TiO_2 and TiO_2-GR composite photocatalysts in dark and under UV light irradiation. The radius of the arc on the EIS spectra reflects the solid state interface layer resistance and the surface charges transfer resistance.[30, 31] In the study of TiO_2-GR composites, EIS spectra are currently used to demonstrate the improved charges separation efficiency induced by graphene.[5, 8, 12, 20, 30] In Fig.5a, the arc radii of TiO_2-GR are smaller than that of TiO_2 in dark, indicating that the introduction of graphene can effectively increase the conductivity of the TiO_2-GR composites and reduce the surface resistance. In Fig.5b, the EIS Nyquist plot arc radii of TiO_2-GR are all smaller than that of TiO_2 under UV light irradiation, which may be attributed to two reasons: (1) improved charges separation efficiency caused by graphene or (2) the introduction of high conductivity graphene can reduce the surface resistance. As can be seen, the arc radii in the plot of TiO_2-GR composites decrease with the increase of

graphene loading amount with and without light irradiation, suggesting that the surface resistance of TiO_2-GR composites decrease gradually with increasing graphene amount. This is because the excellent conductivity of graphene can effectively reduce the surface resistance of composite photocatalyst and promote the migration of electrons. Moreover, TiO_2-8%GR presents the smallest surface resistance, which is in agreement with its optimal H_2 evolution performance. These results indicate that graphene can promote the migration of photo-generated electrons and decrease the surface resistance of TiO_2-GR composites. Because the graphene can only promote the migration of electrons, it can be inferred that if the migration speed of holes is the rate-determining step in the photocatalytic reaction, the graphene combination can't validly enhance the photocatalytic oxidation activity.

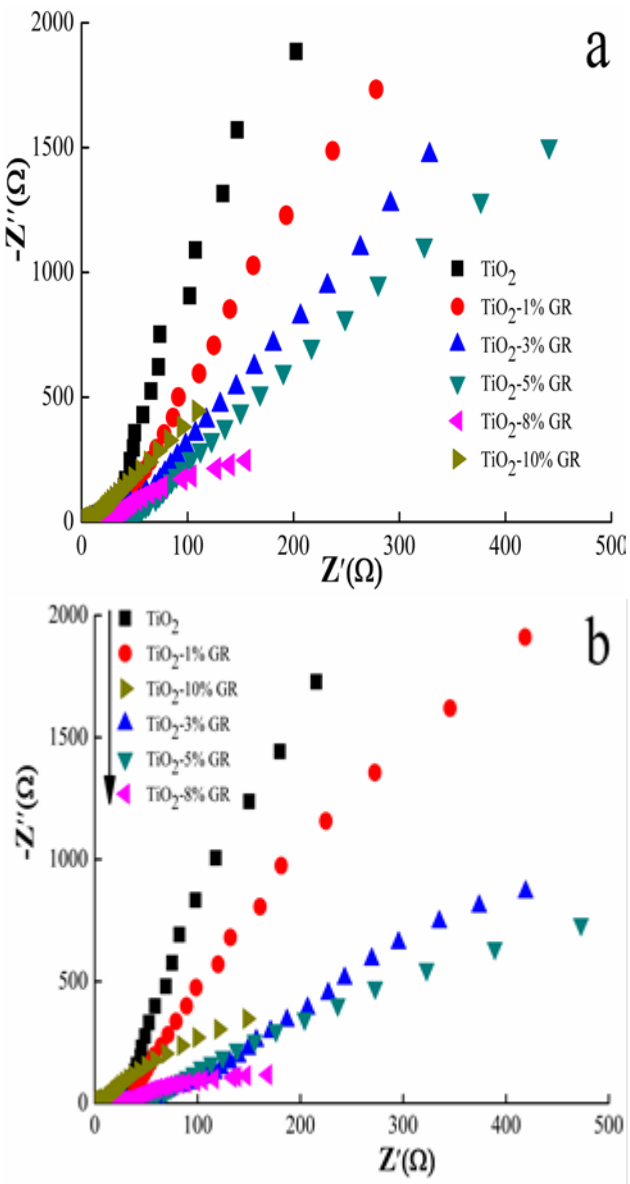

Fig.5 EIS Nyquist plots of TiO_2 and TiO_2-GR composites in dark (a) and under UV irradiation (b)

The detection of main oxidative species in the photocatalytic process is important to reveal the photocatalytic mechanism. In photocatalytic process, there are three main active species: holes, hydroxyl radicals and superoxide radials. The main oxidative species in the photocatalytic process could be examined through the trapping by t-BuOH (hydroxyl radical scavenger), EDTA-2Na (hole scavenger) and N_2 (superoxide radical scavenger).[26, 31, 32] On the degradation of MB, the photocatalytic activity of TiO_2 and TiO_2-GR composites were greatly suppressed by the addition of a scavenger for holes (EDTA-2Na) (Fig. 6). On the contrary, the additions of a scavenger for hydroxyl radicals (t-BuOH) and a scavenger for superoxide radicals (N_2) only cause a small change in the MB degradation. These results suggest that the photo-generated holes are the main oxidative species of the TiO_2 and TiO_2-GR system. Moreover, in phenol degradation, the photo-generated holes are also the main oxidative species of the TiO_2 and TiO_2-GR system. These results are shown in Fig. S6. Therefore, the holes are the key factors in the photocatalytic oxidation reaction in TiO_2 and TiO_2-GR system, the concentration and migration speed of holes are regarded as the rate-determining step in the photo-oxidation reaction.

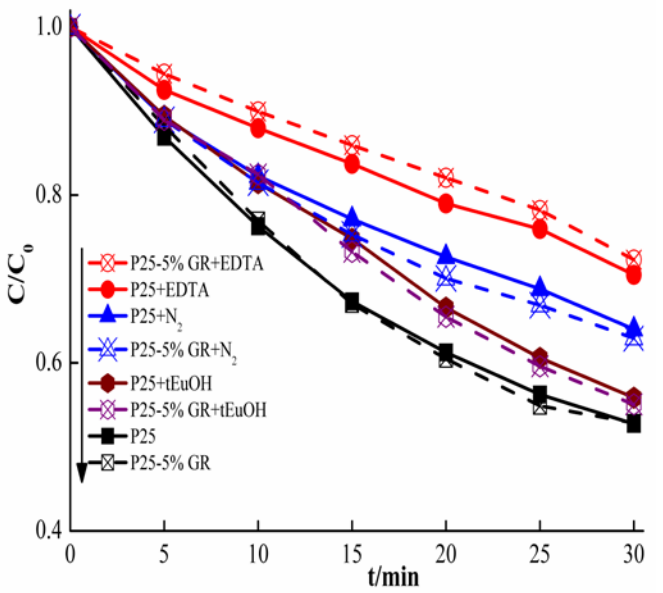

Fig.6 The plots of oxidative species trapping in the system of photodegradation MB over TiO_2 and TiO_2-5%GR composites (MB initial concentration =37.4 ppm, λ= 254 nm)

It is well known that the migration rate of holes is much lower than that of electrons.[33] The main oxidative species of TiO_2 and TiO_2-GR system are photo-generated holes, meaning that the improvement of the migration rate of holes is crucial for increasing the photocatalytic oxidation activity. However, the introduction of graphene only can promote the migration of electrons; thus, introduction of graphene can't effectively enhance photocatalytic oxidation activity (Scheme.1a). The apparent enhancement of photocatalytic oxidation activity in many reports is due to the low reaction initial concentration

caused by strong adsorptivity of graphene for pollutants. In photocatalytic H_2 evolution reduction, the photo-generated electrons on the CB of TiO_2 will transfer into the graphene sheet and subsequently react with the adsorbed H^+ ions to form H_2 (Scheme.1b).[10, 20, 29, 34] The electrons play a major role in photocatalytic H_2 evolution, and graphene acts as a H_2 evolution cocatalyst. Furthermore, the excellent electron mobility and a high surface area of graphene can promote the migration of photo-generated electrons and increase the reaction space,[23] leading to an enhanced H_2 evolution activity.

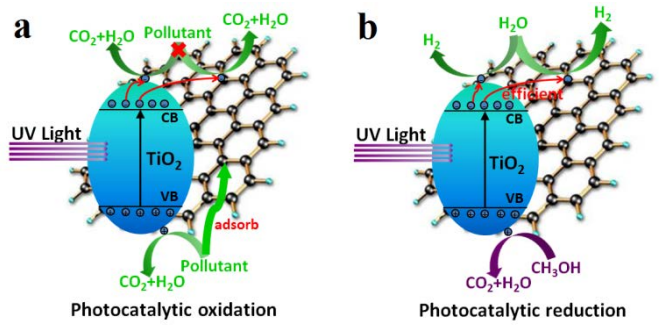

Scheme.1 Schematic drawing illustrating the mechanism of charge transfer in the TiO_2-GR composite under light irradiation

3.3 Structure and morphology of TiO_2-GR composites

Table.1 shows the BET surface area and pore structure of TiO_2 and TiO_2-GR composites. The BET surface area of TiO_2-GR composites gradually increase with increasing graphene amount. The BET surface area of TiO_2-10%GR (80.6 m^2/g) is almost two times as high as that of TiO_2 (46.8 m^2/g), meaning that the adsorption of pollutant over TiO_2-10%GR is greatly enhanced.

Table.1 BET surface area and pore structure of TiO_2 and TiO_2-GR

Samples	SBET(m^2/g)	Pore volume (cm^3/g)
TiO_2	46.8	0.003
TiO_2-1%GR	56.8	0.002
TiO_2-5%GR	67.9	0.002
TiO_2-10%GR	80.6	0.001

Fig.7 shows the TEM images of TiO_2 and TiO_2-GR composites. When the loading amount of graphene is low (TiO_2-1%GR), the graphene sheet can't be observed (Fig.7b). As can be seen, with the increase of graphene loading amount (TiO_2-5%GR and TiO_2-10%GR), the TiO_2 particles were well dispersed on the graphene sheet (Fig.7c and Fig.7d). Part of graphene sheets were blank and didn't interact with TiO_2, which would become the adsorption centre of pollutants during the process of photocatalytic oxidation.[9, 14] However, an appropriate amount of graphene in TiO_2- GR composites is able to promote the migration of electrons and then improve the H_2 evolution.

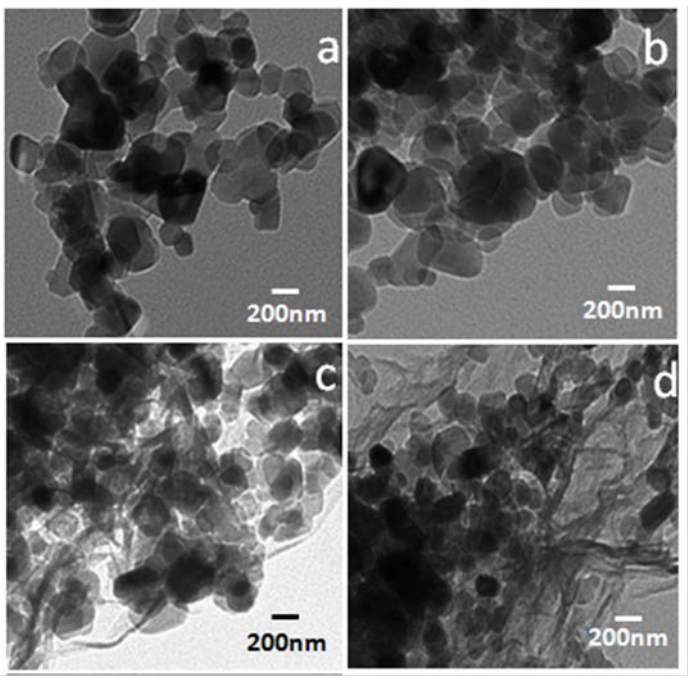

Fig.7 TEM images of TiO_2 and TiO_2-GR composites, (a) TiO_2, (b) TiO_2-1%GR, (c) TiO_2-5%GR, (d) TiO_2-10%GR

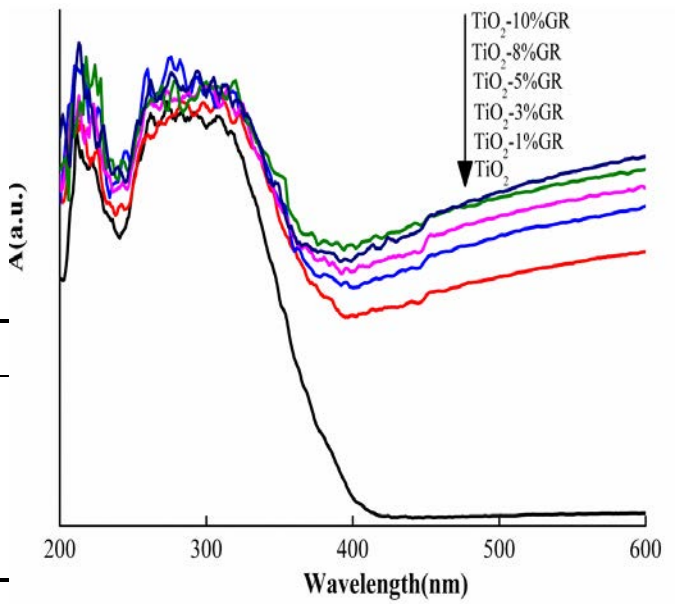

Fig.8 UV-Vis DRS of TiO_2 and TiO_2-GR

The range of light absorption plays a very important role in the photocatalysis.[4, 15, 30] The optical properties of TiO_2 and TiO_2-GR composites were measured by UV-Vis DRS (Fig. 8). TiO_2 exhibit a fundamental absorption edge rises at 400 nm. In TiO_2-GR composites, the addition of graphene induces a continuous background absorption band in the range of 400-800 nm. The background absorption intensity in the range of 400-800 nm of TiO_2-GR increases gradually with the increasing of the graphene amount, which are in agreement with the black color of the samples. It can be observed that there are red shifts

of TiO_2-GR to higher wavelength than TiO_2 in the absorption edge. However, it is it is very difficult to determine the value for such a red shift because the background absorption ranging from 400-800 nm is increased upon the incorporation of graphene into TiO_2.[7]

The Raman spectra of graphene and TiO_2-GR composites were shown in Fig.S7. As can be seen, all samples present two peaks at around 1350 cm^{-1} and 1590 cm^{-1}, which can be attributed to the defects in the hexagonal graphitic layers (D band) and the sp^2 carbon-type structures (G band) respectively. [35, 36] Compared with pure graphene, the peak position of D band and G band of all TiO_2-GR composites show no shift.

4. Conclusions

In this work, TiO_2-GR composites were synthesized via hydrothermal methods in ethanol-water solvent. The role of graphene on the photocatalytic oxidation and photocatalytic reduction of TiO_2-GR composites has been systematically investigated. The pollutant adsorption and degradation results strongly suggest that the composited graphene can't enhance the photocatalytic oxidation performance of TiO_2, the increased apparent rate constant k of TiO_2-GR composite is due to the lower reaction initial concentration caused by strong adsorptivity of graphene for pollutant. In photocatalytic reduction, graphene as a cocatalyst can effectively promote the migration of photo-generated electrons, resulting in an improved H_2 evolution activity. Our finding is expected to avert the misleading message of the effect of graphene and provide new insights on the relationship between the photocatalytic activity and graphene-based photocatslysts.

Acknowledgements

This work was partly supported by National Basic Research Program of China (2013CB632403), National High Technology Research and Development Program of China (2012AA062701) and Chinese National Science Foundation (21437003 and 21373121).

Notes

[a] Department of Chemistry, Beijing Key Laboratory for Analytical Methods and Instrumentation, Tsinghua University, Beijing 100084, P.R. China;
[b] Institute of Aeronautical Meteorology and Chemical Defence, Beijing 100085, P.R. China;
[c] State Key Laboratory of Heavy Oil Processing, China University of Petroleum, Beijing 102249, P.R. China

† Yanyan Zhu and Yajun Wang contributed equally to this work.

Supplementary Information (ESI) available: See DOI: 10.1039/b000000x/

References

1. S. Y. Toh, K. S. Loh, S. K. Kamarudin and W. R. Wan Daud, *Chemical Engineering Journal*, 2014, **251**, 422-434.
2. J. Xu, L. Wang and Y. Zhu, *Langmuir : the ACS journal of surfaces and colloids*, 2012, **28**, 8418-8425.
3. Y. Yang, Y. Xie, L. Pang, M. Li, X. Song, J. Wen and H. Zhao, *Langmuir : the ACS journal of surfaces and colloids*, 2013, **29**, 10727-10736.
4. N. Jiang, Z. X. Xiu, Z. Xie, H. Li, G. Zhao, W. Wang, Y. Wu and X. Hao, *NewJ.Chem.*, 2014, **38**, 4312--4320.
5. Z. Chen, S. Liu, M. Q. Yang and Y. J. Xu, *ACS applied materials & interfaces*, 2013, **5**, 4309-4319.
6. Z. Fang, Y. Wang, J. Song, Y. Sun, J. Zhou, R. Xu and H. Duan, *Nanoscale*, 2013, **5**, 9830-9838.
7. Y. Zhang, Z. Tang, X. Fu and Y. Xu, *ACS Nano*, 2010, **4**, 7303-7314.
8. H. Zhang, X. Lv, Y. Li, Y. Wang and J. Li, *ACS Nano*, 2009, **4**, 380-386.
9. T. Lu, R. Zhang, C. Hu, F. Chen, S. Duo and Q. Hu, *Physical chemistry chemical physics : PCCP*, 2013, **15**, 12963-12970.
10. N. Zhang, Y. Zhang and Y. J. Xu, *Nanoscale*, 2012, **4**, 5792-5813.
11. Y. Liu, Y. Hu, M. Zhou, H. Qian and X. Hu, *Applied Catalysis B: Environmental*, 2012, **125**, 425-431.
12. Z. Chen, N. Zhang and Y. Xu, *CrystEngComm*, 2013, **15**, 3022-3030.
13. Z. Zhang, F. Xiao, Y. Guo, S. Wang and Y. Liu, *ACS applied materials & interfaces*, 2013, **5**, 2227-2233.
14. D. Zhang, X. Pu, G. Ding, X. Shao, Y. Gao, J. Liu, M. Gao and Y. Li, *Journal of Alloys and Compounds*, 2013, **572**, 199-204.
15. P. Wang, J. Wang, X. Wang, H. Yu, J. Yu, M. Lei and Y. Wang, *Applied Catalysis B: Environmental*, 2013, **132-133**, 452-459.
16. J. Li, S. l. Zhou, G.-B. Hong and C.-T. Chang, *Chemical Engineering Journal*, 2013, **219**, 486-491.
17. L. Zhang, H. Li, Y. Liu, Z. Tian, B. Yang, Z. Sun and S. Yan, *RSC Advances*, 2014, **4**, 48703–48711.
18. T.-D. Nguyen-Phan, V. H. Pham, E. W. Shin, H.-D. Pham, S. Kim, J. S. Chung, E. J. Kim and S. H. Hur, *Chemical Engineering Journal*, 2011, **170**, 226-232.
19. X. Hu, G. Li and J. C. Yu, *Langmuir : the ACS journal of surfaces and colloids*, 2010, **26**, 3031-3039.
20. L. Liu, Z. Liu, A. Liu, X. Gu, C. Ge, F. Gao and L. Dong, *ChemSusChem*, 2014, **7**, 618-626.
21. M. Z. Chang K. , Wang Tao, Kang Qing , Ouyang Shuxin , Ye Jinhua *ACS nano*, 2014, **7**, 1078-7087.
22. X. Zhang, H. Li, X. Cui and Y. Lin, *Journal of Materials Chemistry*, 2010, **20**, 2801-2806.
23. Q. Li, B. Guo, J. Yu, J. Ran, B. Zhang, H. Yan and J. R. Gong, *J. Am. Chem. Soc.*, 2011, **133**, 10878-10884.
24. Y. S. Xu, Kaixuan; Li, Chun; Shi, Gaoquan, *ACS Nano*, 2010, **4**, 4324-4330.
25. R. K. Upadhyay, N. Soin and S. S. Roy, *RSC Advances*, 2014, **4**, 3823.
26. Y. Wang, R. Shi, J. Lin and Y. Zhu, *Energy & Environmental Science*, 2011, **4**, 2922-2929.
27. C. Wang, M. Cao, P. Wang and Y. Ao, *Materials Letters*, 2013, **108**, 336-339.
28. M. R. Hoffmann, S. T. Martin, W. Choi and D. W. Bahnemann, *Chemical Reviews*, 1995, **95**, 69-96.
29. S. Morales-Torres, L. M. Pastrana-Martinez, J. L. Figueiredo, J. L. Faria and A. M. Silva, *Environmental science and pollution research international*, 2012, **19**, 3676-3687.
30. M. Zhang, X. Bai, D. Liu, J. Wang and Y. Zhu, *Applied Catalysis B: Environmental*, 2015, **164**, 77-81.
31. Y. Zhu, Y. Liu, Y. Lv, Q. Ling, D. Liu and Y. Zhu, *Journal of Materials Chemistry A*, 2014, **2**, 13041–13048.

32. H. Liu, S. Cheng, M. Wu, H. Wu, J. Zhang, W. Li and C. Cao, *The Journal of Physical Chemistry A*, 2000, **104**, 7016-7020.
33. H. A. Huy, B. Aradi, T. Frauenheim and P. Deák, *Physical Review B*, 2011, **83**, 155201-155207.
34. X. An and J. C. Yu, *RSC Advances*, 2011, **1**, 1426-1434.
35. G. Wang, J. Yang, J. Park, X. Gou, B. Wang, H. Liu and J. Yao, *The Journal of Physical Chemistry C*, 2008, **112**, 8192-8195.
36. S. Stankovich, D. A. Dikin, R. D. Piner, K. A. Kohlhaas, A. Kleinhammes, Y. Jia, Y. Wu, S. T. Nguyen and R. S. Ruoff, *Carbon*, 2007, **45**, 1558-1565.

